STRETCHED-FILM MICROMIRRORS FOR IMPROVED OPTICAL FLATNESS

Jocelyn T. Nee, Robert A. Conant, Matthew R. Hart, Richard S. Muller, and Kam Y. Lau
Berkeley Sensor & Actuator Center, University of California
497 Cory Hall, Berkeley, CA, 94720-1770, USA

ABSTRACT

We have developed a new tensile optical-surface (TOS) process to produce optically flat micromirrors capable of scanning at high frequencies. A polysilicon membrane is stretched across a stiff, single-crystal silicon-rib structure. This structure increases the stiffness of the mirror without significantly increasing its mass. The low mass makes possible high operating frequencies without deformation that could significantly compromise the optical performance of the mirror. Electrostatic combdrives, made of thick single-crystal silicon, provide large forces that enable mirror operation at tens of kHz.

INTRODUCTION

Many optical-MEMS applications depend on surfaces that are flat to within λ/4 or better (about 140 nm for visible wavelengths.) However, scanning micromirrors that are fabricated using polysilicon surface-micromachining processes (for example the MCNC Multi-User MEMS Process (MUMPS)) have shown nonplanar mirror deformations of 1-2 μm [1-2]. These deformations are not a problem for many mechanical systems, but they can seriously degrades optical performance. Suggested ways to avoid deformations include: 1) using bulk micromachining to produce a flat, but comparatively thick, single-crystal silicon mirror [3], and 2) using planarization methods such as chemical-mechanical polishing (CMP) to make flat, thin-film mirrors [4]. Each of these methods has disadvantages. The thick single-crystal silicon mirrors have relatively large mass and therefore require actuators capable of exerting forces large enough to drive heavy loads. The surface-micromachined mirrors are lightweight, but they are not stiff enough to remain planar when damped by inertial forces imposed by high-frequency scanning [5-6].

In order to make a light, stiff mirror capable of high-speed scanning which retains optical flatness, we have developed a new bulk-/surface-micromachining hybrid-fabrication process that makes use of both the flatness achievable with bulk-micromachining and the low mass achievable with surface micromachining. We describe a tensile optical surface (TOS) mirror structure and the associated fabrication process. We also show measurements of static deformations of the fabricated mirrors, and predict dynamic deformations using modal analysis.

STRUCTURAL DESIGN

Tensile Optical-Surface (TOS) micromirrors

The tensile optical-surface (TOS) micromirrors are designed to be both lightweight and stiff. They are made of tensile membranes of polysilicon supported by stiff, circular single-crystal-silicon support ribs (Figure 1). The mirror structure is like that of a drum – the reflecting surface is tensile and stretches flat across the stiff support rib. A thin layer of gold can be evaporated onto its surface to increase its reflectivity.

The 550 μm-diameter membrane has a resonant frequency in the hundreds of kHz, which allows the mirror to be scanned at tens of kHz without significantly exciting membrane resonant modes that would compromise its planarity.

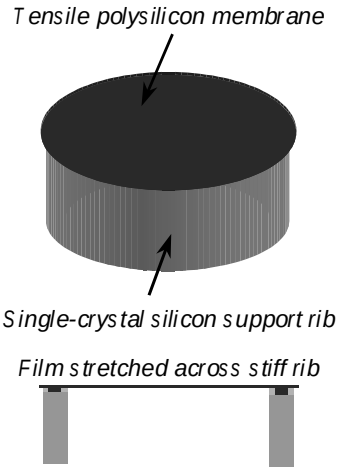

Figure 1: Schematic of the stretched optical-surface mirror design. A stiff circular rib made of single-crystal silicon supports the polysilicon-mirror membrane.

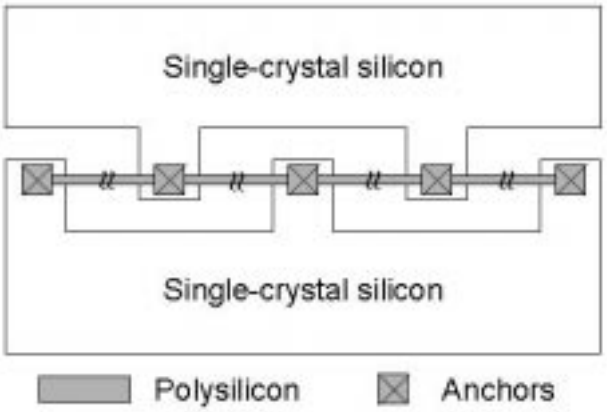

Figure 2: Top-view sketch showing folding hinges, a series of long polysilicon beams attached at multiple anchoring points to the single-crystal silicon areas.

Folding hinge design

The TOS process allows structures to be built that can be folded out of the substrate plane using hinges made in the polysilicon layer. A set of long polysilicon beams connects the two single-crystal-silicon areas, as shown in Figure 2. The polysilicon beams are typically 100–200 μm long and 3–5 μm wide and twist to allow the plates to fold up.

FABRICATION PROCESS

The TOS process begins with a silicon-on-insulator wafer (Bondtronix, Inc.) having a top single-crystal silicon layer that is 15 μm thick. In the finished device, the mirror rib, a support frame, and the electrostatic combdrive are all fabricated from this single-crystal silicon layer. The mirror membrane and the hinges are made from an LPCVD-deposited tensile polysilicon layer.

The fabrication sequence for the TOS micromirror is illustrated in Figure 3. Using a deep reactive-ion etching (DRIE) system, we etch holes into the top silicon layer at the sites at which it will later be anchored to the substrate. We also etch away the silicon dioxide from the bottom of the holes. We next deposit a 1.5 μm-thick low-stress silicon nitride layer, which anchors the top silicon layer to the substrate, and also acts as an etch stop layer for a subsequent chemical-mechanical polishing (CMP) step.

In the next step, we etch trenches underneath the mirrors and hinges. We then deposit LPCVD polysilicon and thermally oxidize the polysilicon to obtain a conformal silicon dioxide layer which fills the trenches [7] Using CMP, we planarize the surface and then deposit 1.5 μm-thick LPCVD fine-grained polysilicon at 590°C. Guckel

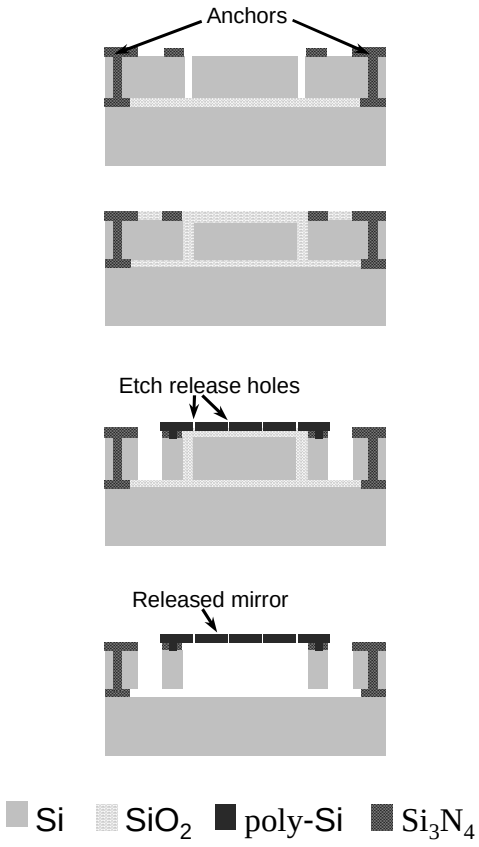

Figure 3: Cross sections showing the TOS mirror-fabrication process sequence.

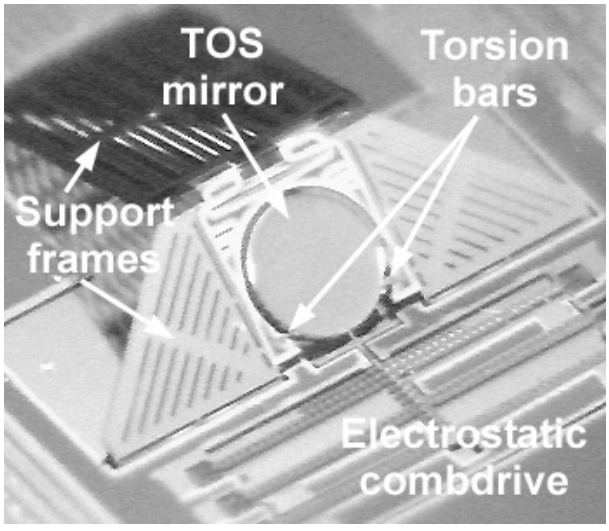

Figure 4: TOS mirror and support structure after release and assembly. The 550 μm-diameter TOS mirror is mounted on support frames via torsional hinges, and is driven by an electrostatic combdrive.

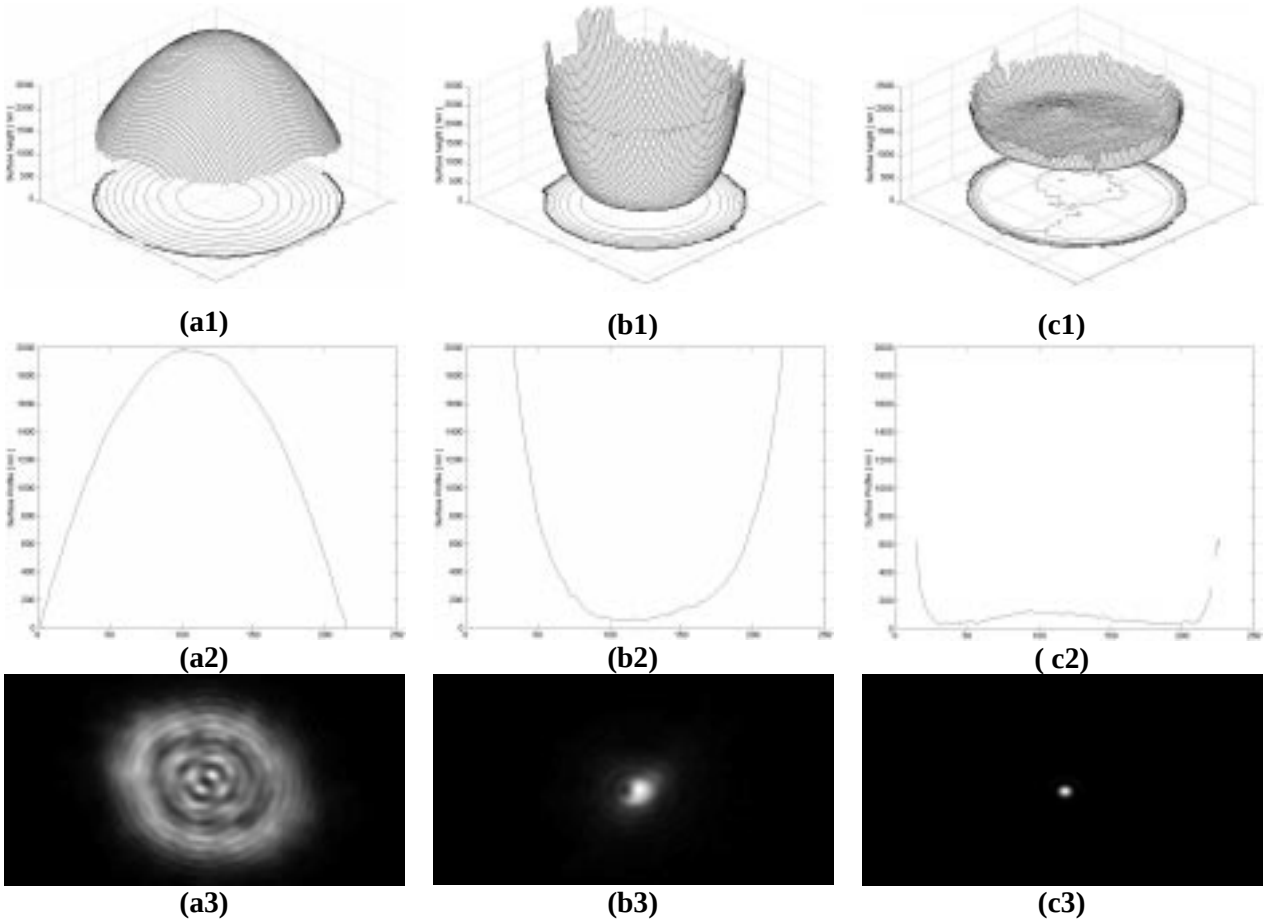

Figure 5: Surface height profile (1) and cross-sectional views (2) of the surfaces of 550 μm-diameter micromirrors fabricated using a) MUMPS process, b) TOS process, and c) TOS process with non-SOI wafer. (3) shows the calculated far-field intensity distribution of the reflected beam if a collimated beam of light were incident on the mirror.

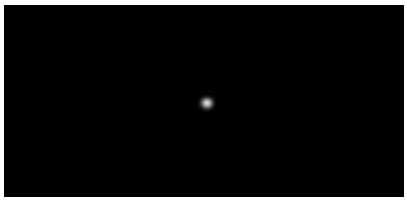

Figure 6: Calculated far-field intensity distribution of the reflected beam if a collimated beam of light were incident on a perfect, diffraction-limited mirror 550 μm in diameter.

et. al. [8] have shown that post-deposit anneal of the polysilicon film at moderate temperatures ranging between 650°C and 950°C yields tensile stress in the polysilicon film. For our process, the stress of the polysilicon film, as deposited, is 336 MPa tensile, measured using stress test structures built in the same process. Subsequent anneals using rapid thermal annealing (RTA) in nitrogen between the temperatures of 750°C and 900°C produced films with stresses ranging between 300 and 100 MPa respectively. A second DRIE etch of the single-crystal silicon layer defines the remainder of the structures, including the mirror-support frames and the electrostatic combdrives. The mirrors are released in a 49% hydrofluoric acid solution and dried using a supercritical carbon dioxide chamber [9]. Figure 4 shows a mirror after release and assembly.

RESULTS

We made 550-μm-diameter mirrors, with 1.5 μm-thick films of polysilicon stretched over 15 μm-tall and 13 μm-wide ribs. The stress of the polysilicon film is measured to be 336 MPa tensile using stress test structures built in the same process.

Static mirror curvature

Figure 5(a) shows the static curvature in a 550 μm-diameter, 1.5 μm-thick non-TOS (MUMPS-fabricated) mirror, measured using phase-shifting interferometry [5]. The total peak-to-valley surface deformation is approximately 2 μm. The calculated far-field intensity pattern for an optical beam reflected from this mirror is shown in Figure 5(a3), and Figure 6 shows the calculated far-field-intensity pattern reflected from a perfectly planar mirror of the same size to provide a reference.

For a scanning mirror with a given scan angle, the size of the reflected spot determines the number of resolvable spots per line, or equivalently the resolution of the scanner. The larger is the spot, the smaller is the number of resolvable spots per line. Thus, the large spot size of the MUMPS mirror causes the scanner to have very low resolution.

Figure 5(b) shows measured results from the TOS mirror. The central portion of the mirror is relatively flat (less than 500 nm deformation over 70% of the cross section), and there is a sharp change in curvature near the mirror edge. The far-field-intensity distribution is significantly smaller when compared to that of the MUMPS mirror.

Since the surface deformation of the TOS mirror shown in Figure 5(b) is likely due to bending of the support rib as a result of tensile stress in the membrane, we have also included results from a TOS mirror fabricated on a non-SOI wafer. This mirror is fabricated in the same process run as that producing the TOS mirror, with the only difference being that the starting wafer is single-crystal silicon rather than an SOI wafer. On the single-crystal silicon wafer, the optical surface is the same, but the support ribs are part of the silicon-substrate wafer and fold out is not possible. This mirror shows significantly less surface deformation – only about 0.1 μm across the center portion of the mirror, as shown in Figure 5(c). The far-field-intensity distribution also shows significant improvement over the mirrors shown in Figures 5(a) and 5(b).

We can modify several process parameters to improve the performance of the TOS mirror by decreasing its static curvature. Specifically, by increasing the thickness of the top silicon layer of the SOI wafer (and therefore the height of the rib) and by decreasing the tensile stress in the polysilicon film using higher temperature annealing, we can obtain flatter mirrors. Increasing the rib width and decreasing the membrane thickness will also help to decrease static curvature.

Dynamic deformation analysis

To investigate the effects of dynamic deformation, we have performed finite-element analysis (FEA) simulations to determine the mirror-mode shapes and resonant frequencies. We performed modal analysis on TOS mirror "drum" structures having the same dimensions as those fabricated and having differing tensile stress values in the top polysilicon layers. For comparison, modal analysis is also carried out for a circular polysilicon plate having the same hinge dimensions, mirror diameter and mass moment-of-inertia about the same axis-of-rotation as the drum structure. The thickness of the simulated plate is 4 μm.

Figure 7 illustrates the four lowest-frequency modes that are excited when a force is applied to the bottom point of the structure, as in the case of driving the mirror with an electrostatic combdrive attached there. Tilting is the desired operating mode, any other modes (all of higher order) are undesired and their excitation would reduce optical resolution in the scanning mirror system.

We can estimate the amount of energy that is coupled into each of the undesired higher-order modes using the following steady-state analysis.

Let the normalized eigenvectors, or modes, of the system be $\boldsymbol{u}_i$, and the first element of each eigenvector be $\boldsymbol{u}_i(1)$. The eigenvalues are $\lambda_i = \omega_i^2$, where ω_i is the resonant frequency of the i^{th} mode. Let **U** be an array of the N eigenvectors, i.e. $\mathbf{U} = [\boldsymbol{u}_1\ \boldsymbol{u}_2\ \boldsymbol{u}_3\ \ldots\ \boldsymbol{u}_N]$. The transpose of

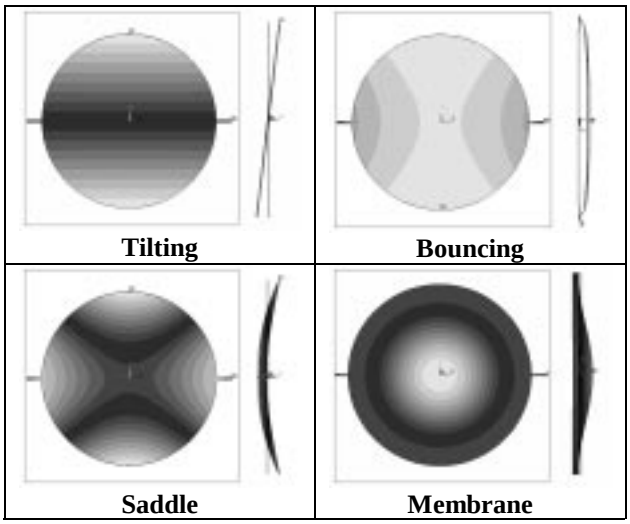

Figure 7: Sample mode shapes (top and edge views) of the plate and drum structures from FEM analysis. These modes may be excited when force is applied to the bottom point of the structure to tilt it.

this transformation matrix is equal to its inverse, i.e. $\mathbf{U}^{\mathbf{T}} = \mathbf{U}^{-1}$.

The equation of motion is

$$\mathrm{M}\,\ddot{x} + \mathrm{C}\,\dot{x} + \mathrm{K}\,x = F \tag{1}$$

where **M** is the mass matrix, **C** is the damping matrix, **K** is the stiffness matrix, ***F*** is the applied force, and ***x*** is the displacement of the system measured at the force-coupling point. When we transform to the modal coordinate system using eigenvector matrix **U** (so $\boldsymbol{x} = \mathbf{U}\boldsymbol{p}$), then the transformed equation of motion becomes

$$\ddot{p} + \mathrm{U}^{\mathrm{T}}\mathrm{C}\mathrm{U}\,\dot{p} + \Lambda\,p = \mathrm{U}^{\mathrm{T}}\,F \tag{2}$$

where $\mathbf{\Lambda}$ is a diagonal matrix with the eigenvalues λ_i on the diagonal.

If force is applied only at node 1, i.e. $\boldsymbol{F} = [1\ 0\ 0\ \ldots\ 0]^T$, then $\mathbf{U}^{\mathbf{T}}\boldsymbol{F} = [\boldsymbol{u_1}(1)\ \boldsymbol{u_2}(1)\ \boldsymbol{u_3}(1)\ \ldots\ \boldsymbol{u_N}(1)]^{\mathrm{T}}$ is the force vector in the transformed coordinate system. In steady state, $\ddot{p} = \dot{p} = 0$, so

$$p = \left[u_1(1)\omega_1^2, u_2(1)\omega_{21}^2, \ldots, u_n(1)\omega_{n1}^2,\right]^T \tag{3}$$

Equation (3) can be transformed into the original coordinate system using the transformation matrix **U**, so

$$x = \sum_{i=1}^{\infty} \frac{u_i(1)}{\omega_i^2} u_i \tag{4}$$

Thus, if a mode has zero displacement at node 1, then $\boldsymbol{u_i}(1)$ is zero and that mode does not appear in the solution. Those modes that do show up in the solution are scaled by a factor of $1/\omega_i^2$. This result indicates that modes at higher frequencies have smaller magnitude, and thus contribute much less to the overall shape of the structure than do lower frequency modes.

Using this method, we estimate the total contribution of higher-order modes to the overall shape of the structure for three cases: a circular polysilicon plate 4 μm in thickness, a drum structure with zero stress in the membrane, and a drum structure with 336 MPa stress (as found in the fabricated structure). For a ±15° optical scan, the motion of the tilting mode must be 36 μm. By scaling the other modes as described above, we determine the total deviations from planarity expected for the mirror structures. We summarize these in Table 1. For the 4μm-thick plate, the nonplanarity is 367 nm. The drum structure with no stress in the polysilicon still has 111 nm of nonplanar deformation. On the other hand, the drum structure with the high tensile stress in the polysilicon membrane has modes with far higher resonant frequencies, so these higher-order modes contribute less than 55 nm of nonplanar deformation.

DISCUSSION

The requirements governing the process parameters for making the TOS mirror are set by the need to minimize static- and dynamic-deformation of the mirror surface while, at the same time, minimizing the mass moment-of-inertia about the axis-of-rotation. To minimize static deformations, the TOS mirrors should have small membrane residual stress and tall ribs. To minimize

	Plate: 4 μm thick		**Drum: 0 MPa stress**		**Drum: 336 MPa stress**	
Mode	**Resonant Frequency (kHz)**	**Nonplanar Contribution**	**Resonant Frequency (kHz)**	**Nonplanar Contribution**	**Resonant Frequency (kHz)**	**Nonplanar Contribution**
Tilting	2.830	0 nm	2.843	0 nm	3.008	0 nm
Bouncing	18.963	321 nm	25.869	91 nm	69.868	45 nm
Saddle	119.240	36 nm	205.691	14 nm	173.631 304.960	3 nm
Membrane	176.580	10 nm	92.902 174.652	6 nm	217.500	6 nm
Total nonplanar contribution		367 nm		111 nm		54 nm

Table 1: Modal frequencies and contributions of each mode to the final shape of the mirror given an excitation at the bottom point of the mirror which causes the mirror to move 36 μm in the tilting mode (corresponding to a ±15° optical scan.) Calculations in steady-state for three different cases: 1) circular plate with uniform thickness of 4 μm, 2) drum structure with zero stress in the membrane, and 3) drum structure with 336Mpa stress in the membrane.

dynamic deformation, however, we must raise the frequencies of high-order modes, indicating that higher membrane stresses are desirable.

Design for high-speed scanning

To design structures that are suitable for high-speed scanning, we should use a thick top silicon layer and a moderate- to high-tensile-stress polysilicon film. The thick top silicon layer will yield both tall support ribs for the TOS mirror and thick combdrives. The tall support ribs and the high tensile stress in the polysilicon film increases the stiffness of the TOS drum structure, thus allowing the mirror to be operated at high frequencies with little deformation. The thick combdrives will provide the large actuation force necessary . For high frequency operation, the system spring stiffness can be increased by 1) using the single-crystal silicon layer (rather than the polysilicon layer) for the mirror torsion hinges, 2) moving the torsion hinges closer to the bottom of the mirror (thus increasing their effective stiffness,) and 3) decreasing the length of the restoring springs of the electrostatic combdrive.

Design for low-voltage, low-frequency operation

For dc or low-frequency operation, it is desirable to work at low voltages. For low-voltage operation, it is important to decrease the overall stiffness in the hinges but still maintain low-mass and high-force actuators. We can achieve this by having a thick top silicon layer and thin membranes with low tensile stress. A thin membrane with lower stress will decrease the stiffness of the torsion hinge, while the thicker rib will maintain the stiffness of the mirrors. Thick combdrives with loose springs will make good high-force actuators for low-voltage dc operation.

CONCLUSIONS

We have described a new tensile optical-surface (TOS) process to make optically flat, high-speed micromirrors. A polysilicon membrane is stretched across a stiff, single-crystal silicon-rib structure resulting in a reflecting surface that is under tension. The drum structure of the TOS mirror allows the mirror to have high stiffness and low mass moment-of-inertia. Compared to typical thin-film micromirrors, the TOS micromirror offers an order-of-magnitude improvement in its achievable optical resolution. With the capability of making stiff mirrors having small mass moment-of-inertia and high-force actuators in the same fabrication run, the TOS process provides a means to produce micromirrors for high-frequency scanning as well as low-voltage dc or low-frequency operation.

ACKNOWLEDGMENTS

This work is supported under DARPA grant contract number DABT-63-95-C-0055 and NSF grant contract number EEC-9615774.

REFERENCES

[1] P.M. Hagelin, U. Krishnamoorthy, R. Conant, R. Muller, K. Lau, and O. Solgaard, “Integrated micromachined scanning display systems,” presented at 18th Congress of ICO, San Francisco, CA, August 1999, pp.472-3.

[2] P.M. Hagelin and O. Solgaard, “Optical raster-scanning displays based on surface-micromachined polysilicon mirrors,” JSTQE, vol.5, no.1, p.67-74.

[3] S. Kurth, R. Hahn, C. Kaufmann, K. Kehr, J. Mehner, U. Wollmann, W. Dotzel, and T. Gessner, “Silicon mirrors and micromirror arrays for spatial laser beam modulation,” Sensors & Actuators A (Physical), vol.A66, no.1-3, pp.76-82.

[4] D.L. Hetherington and J.J. Sniegowski, “Improved polysilicon surface-micromachined micromirror devices using chemical-mechanical polishing,” Proc. SPIE, vol.3440, pp.148-53.

[5] M. Hart, R.A. Conant, K.Y. Lau, R.S. Muller, “Time-resolved measurement of optical MEMS using stroboscopic interferometry,” Proc. Transducers '99, Sendai, Japan, June 1999, pp. 470-473. (Manuscript submitted to and under review by IEEE/ASME JMEMS)

[6] R.A. Conant, P.M. Hagelin, U. Krishnamoorthy, O. Solgaard, K.Y. Lau, R.S. Muller, “A full-motion video display using micromachined scanning micromirrors,” Proc. Transducers '99, Sendai, Japan, June 1999, pp. 376-379.

[7] C. Keller, *Microfabricated High Aspect Ratio Silicon Flexures*, MEMS Precision Instruments, 1998.

[8] H. Guckel, D.W. Burns, C.C.G. Visser, H.A.C. Tilmans, and D. Deroo, “Fine-grained polysilicon films with built-in tensile strain,” IEEE Trans. Elec. Dev., vol.35, no.6, pp.800-1.

[9] G.T. Mulhern, D.S. Soane and R.T. Howe, “Supercritical Carbon Dioxide Drying of Microstructures,” Transducers ’93, pp. 296-9.